**Liquid Crystals**
Publication details, including instructions for authors and subscription information:
http://www.informaworld.com/smpp/title~content=t713926090

# Thermotropic mesomorphism in penta- and hepta-coordinated metal complexes

Iolinda Aiello[a]; Mauro Ghedini[a]; Annarita Grisolia[a]; Daniela Pucci[a]; Oriano Francescangeli[b]
[a] Centro di Eccellenza CEMIF.CAL - LASCAMM, Unità INSTM della Calabria, Dipartimento di Chimica, Università della Calabria, I-87036 Arcavacata (CS), Italy [b] Dipartimento di Fisica e Ingegneria dei Materiali e del Territorio e Istituto Nazionale per la Fisica della Materia, Università di Ancona, Via Brecce Bianche, I-60131 Ancona, Italy

**To cite this Article** Aiello, Iolinda , Ghedini, Mauro , Grisolia, Annarita , Pucci, Daniela and Francescangeli, Oriano(2005) 'Thermotropic mesomorphism in penta- and hepta-coordinated metal complexes', Liquid Crystals, 32: 6, 763 — 769
**To link to this Article: DOI:** 10.1080/02678290500139328
**URL:** http://dx.doi.org/10.1080/02678290500139328

*Liquid Crystals*, Vol. 32, No. 6, June 2005, 763–769

Taylor & Francis
Taylor & Francis Group

# Thermotropic mesomorphism in penta- and hepta-coordinated metal complexes

IOLINDA AIELLO†, MAURO GHEDINI*†, ANNARITA GRISOLIA†, DANIELA PUCCI† and ORIANO FRANCESCANGELI‡

†Centro di Eccellenza CEMIF.CAL - LASCAMM, Unità INSTM della Calabria, Dipartimento di Chimica, Università della Calabria, I-87036 Arcavacata (CS), Italy
‡Dipartimento di Fisica e Ingegneria dei Materiali e del Territorio e Istituto Nazionale per la Fisica della Materia, Università di Ancona, Via Brecce Bianche, I-60131 Ancona, Italy

(*Received 3 August 2004; in final form 6 January 2005; accepted 13 January 2005*)

New Ni(II) and $UO_2$(II) metallomesogens obtained from mesomorphic *N*,*N′*-salicyliden(3,3′-diamine-*N*-methyldipropylamine) ligands containing a pentadentate $N_3O_2$ chelating cavity and bearing two or four lateral substituents, are isolated and fully characterized. Some of the synthesized nickel and dioxouranium complexes show a SmC mesophase. To the best of our knowledge, these species are the first pentacoordinated Ni(II) and heptacoordinated $UO_2$(II) metallomesogens to be reported.

## 1. Introduction

The molecular geometry imposed by a metal coordination sphere can be a useful tool in obtaining mesomorphic species (metallomesogens) with unusual molecular shapes and related physical properties [1]. Nevertheless, excluding the lanthanide species recently reviewed by Binnemans and Görller-Walrand [2], most of the reported liquid crystalline d-block metal complexes exhibit a square planar coordination geometry [1], while those with coordination number (c.n.) exceeding four are limited to a few species of trigonal bipyramidal (TPY), square pyramidal (SPY) and octahedral (O) geometries. Representative examples of these type of metallomesogen are the derivatives containing the fragments $Fe(CO)_3$, (TPY, [3]), $Zn(NO_3)_2$ (TPY, [4]), $MCl_2$ ($M$=Mn, Ni, Zn; TPY, [5]), VO(IV), (SPY, [6]), $M(CO)_4$ ($M$=Mn, Re; O, [7]) and $PtI_2$(IV) (O, [8]). The influence of an 'odd' metal c.n., on the thermal behaviour in metal complexes is therefore studied here, using mesogenic and pro-mesogenic chelating ligands containing a pentadentate cavity.

Rod-like disubstituted *N*,*N′*-salicylidenediaminato nickel, copper and oxovanadium complexes exhibiting rod-like [9] or forked lateral-tailed [10] molecular shapes were recently examined; the nickel complexes where *N*,*N′*=1,2-diaminoethane or 1,3-diaminopropane showed lower transition temperatures and wider mesomorphic ranges. These *N*,*N′*-salicylidenediaminate tetradentate $N_2O_2$ chelating ligands are easily synthesized from the appropriate substituted salicylaldehydes. Therefore, pentadentate ligands similar to the $N_3O_2$ bonding species arising from 3,3′-diamino-*N*-methyldipropylamine, $CH_3N[(CH_2)_3NH_2]_2$, have been synthesized and their coordination ability tested against Ni(II) and UO(II) metal ions.

The ligand *N*,*N′*-salicyliden(3,3′-diaminate-*N*-methyldipropylamine), $CH_3N[(CH_2)_3N{=}CH(OH)C_6H_4]_2$, gives rise to a stable high spin paramagnetic Ni(II) complex in which the metal ion is penta-coordinated in a distorted TPY geometry. The equatorial positions are occupied by the nitrogen atom bearing the $CH_3$ group and by the two oxygen atoms [11, 12]. In addition, the dioxouranium(VI) ion is known to form hepta-coordinated complexes with both $N_2O_3$ and $N_3O_2$ ligands. In these complexes the linear $[O{=}U{=}O]^{2+}$ cation is usually found perpendicular to the plane containg the O and N set of donating atoms [13]. Therefore, from the reaction between Ni(II) and $UO_2$(II) salts and pro-mesogenic ligands containing the $N_3O_2$ chelating core penta- and hepta-coordinated complexes are expected to be formed. Here we report the synthesis and thermal behaviour of the nickel and dioxouranium complexes obtained from the *N*,*N′*-salicylidenediaminates $\mathbf{H_2L_{1-4}}$ shown in figure 1.

---

*Corresponding author. Email: m.ghedini@unical.it

*Liquid Crystals*
ISSN 0267-8292 print/ISSN 1366-5855 online © 2005 Taylor & Francis Group Ltd
http://www.tandf.co.uk/journals
DOI: 10.1080/02678290500139328

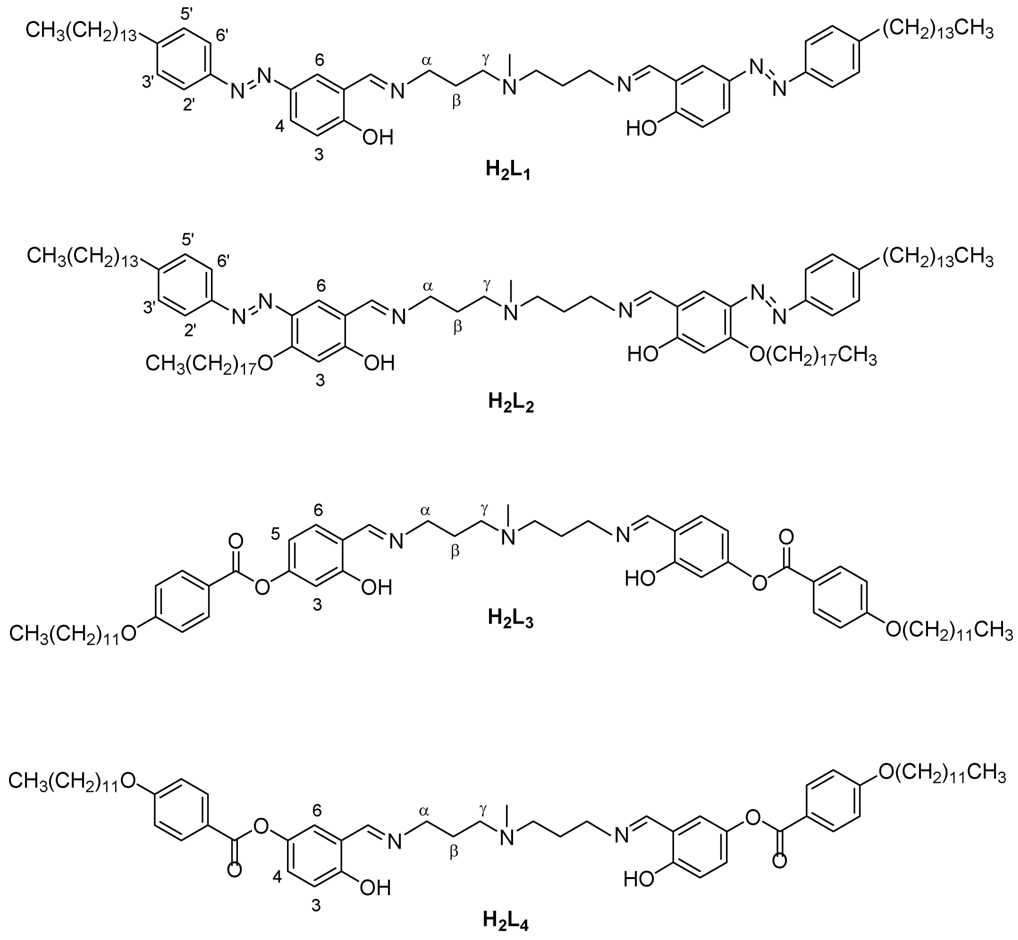

Figure 1. Chemical structure and proton numbering scheme for **H$_2$L$_{1–4}$** ligands.

## 2. Experimental

### 2.1. *General*

Infrared spectra were recorded on a Perkin-Elmer Spectrum One FTIR spectrometer equipped for reflectance measurements. $^1$H NMR spectra were recorded on a Bruker WH-300 spectrometer in CDCl$_3$ solutions, with TMS as internal standard. Elemental analyses were performed with a Perkin-Elmer 2400 analyser, and optical observation were made with a Zeiss Axioscope polarizing microscope equipped with a Linkam C0 600 heating stage. Transition temperatures and enthalpies were measured on a Perkin-Elmer DSC-6 differential scanning calorimeter with a heating and cooling rate of 10.0°C min$^{-1}$ following calibration with indium. The X-ray powder diffraction patterns were obtained using a Bruker AXS general area detector diffraction system (D8 Discover with GADDS). Monochromatized CuK$_\alpha$ radiation ($\lambda$=1.54 Å) impinged on the ~1 mm thick sample, the temperature of which was controlled to ±0.1° by a hot stage containing electrical resistors.

All chemicals were reagent grade and used as purchased without further purification.

### 2.2. *Synthesis of the H$_2$L$_{1–4}$ ligands*

The compounds 2-hydroxy-5-{[4-(*n*-tetradecyl)phenyl] azo}benzaldehyde (**I**) [9] and 2-hydroxy-4-(*n*-octadecyloxy)-5-{[4-(n-tetradecyl)phenyl]azo}benzaldehyde (**II**) [10] were synthesized as previously described. The preparation of 4-dodecyloxybenzoic acid 4-formyl-3-hydroxyphenyl ester (**III**) and 5-dodecyloxybenzoic acid 4-formyl-3-hydroxyphenyl ester (**IV**) was accomplished by modifying the reported literature procedures [14]. The elemental analysis data for all the complexes are listed in table 1.

**2.2.1. Preparation of** H$_2$L$_1$**.** A solution of *N*,*N'*-bis(3-aminopropyl)methylamine (0.09 g, 0.10 ml, 0.59 mmol) and **I** (0.5 g, 1.18 mmol) in methanol (15 ml) was stirred under reflux for 4 h. The precipitate that formed on cooling to room temperature was filtered and washed

Table 1. Elemental analysis for $\mathbf{H_2L_{1-4}}$, $\mathbf{UO_2L_{1-2}}$ and $\mathbf{NiL_{1-2}}$ compounds.

| Compound | Molecular formula | Required (found)/% | | |
|---|---|---|---|---|
| | | C | H | N |
| $\mathbf{H_2L_1}$ | $C_{61}H_{91}N_7O_2$ | 76.76 (76.48) | 9.61 (9.64) | 10.27 (10.38) |
| $\mathbf{H_2L_2}$ | $C_{97}H_{163}N_7O_4$ | 78.12 (78.35) | 11.02 (11.34) | 6.57 (6.87) |
| $\mathbf{H_2L_3}$ | $C_{59}H_{83}N_3O_4$ | 73.64 (73.91) | 8.69 (8.75) | 4.37 (4.28) |
| $\mathbf{H_2L_4}$ | $C_{97}H_{163}N_7O_4$ | 73.64 (73.99) | 8.69 (8.79) | 4.37 (3.98) |
| $\mathbf{UO_2L_1}$ | $C_{61}H_{91}N_7O_4U$ | 59.93 (59.79) | 7.34 (7.48) | 8.02 (8.38) |
| $\mathbf{UO_2L_2}$ | $C_{97}H_{161}N_7O_6U$ | 66.22 (66.54) | 9.22 (9.58) | 5.57 (5.71) |
| $\mathbf{UO_2L_3}$ | $C_{59}H_{81}N_3O_{10}U$ | 57.60 (57.29) | 6.64 (6.51) | 3.42 (3.69) |
| $\mathbf{UO_2L_4}$ | $C_{59}H_{81}N_3O_{10}U$ | 57.60 (57.92) | 6.64 (6.97) | 3.42 (3.22) |
| $\mathbf{NiL_1}$ | $C_{61}H_{89}N_7O_2Ni$ | 72.46 (72.23) | 8.87 (8.75) | 9.70 (9.85) |
| $\mathbf{NiL_2}$ | $C_{97}H_{161}N_7O_4Ni$ | 75.26 (75.54) | 10.48 (10.51) | 6.33 (6.42) |
| $\mathbf{NiL_3}$ | $C_{59}H_{81}N_3O_8Ni$ | 69.54 (69.44) | 8.01 (8.10) | 4.12 (3.80) |
| $\mathbf{NiL_4}$ | $C_{59}H_{81}N_3O_8Ni$ | 69.54 (69.99) | 8.01 (8.09) | 4.12 (4.22) |

with ethanol. The crude product was purified by recrystallization from ethanol and then dried *in vacuo* to a yellow solid; yield 0.51 g (90%). IR (KBr, $cm^{-1}$) $v$: 2954–2850 (stretching aliphatic CH), 1635 (stretching C=N), 1604, 1467. $^1$H NMR ($CDCl_3$, ppm) $\delta$: 14.26 (s, 2H, OH), 8.42 (s, 2H, CH=N), 7.95 (dd, 2H, $J_{4,6}$=2.43 Hz/$J_{3,4}$=8.79 Hz, $H^4$), 7.85 (d, 2H, $J$=2.43 Hz, $H^6$), 7.77 (d, 4H, $J$=8.31 Hz, $H^{2',6'}$), 7.28 (d, 4H, $J$=8.31 Hz, $H^{3',5'}$), 7.03 (d, 2H, $J$=8.79 Hz, $H^3$), 3.70 (t, 4H, $J$=6.33 Hz, $CH_2^{\alpha}$), 2.66 (t, 4H, $J$=7.32 Hz, Ph–$CH_2$), 2.48 (t, 4H, $J$=6.84 Hz, $CH_2^{\gamma}$), 2.25 (s, 3H, $NCH_3$), 1.95–1.05 (m, 52H, aliphatic protons), 0.88 (t, 6H, $J$=6.36 Hz, $CH_3$). The thermal behaviour is reported in table 2.

### 2.2.2. Preparation of $H_2L_2$.

$\mathbf{H_2L_2}$ was prepared by reacting *N*,*N*-bis(3-aminopropyl)methylamine and **II** in methanol (reflux, 4 h). The crude product was purified by recrystallization from chloroform/ethanol and then dried *in vacuo* to yield an Orange solid; yield 0.45 g (83%). IR (KBr, $cm^{-1}$) $v$: 2956–2850 (stretching aliphatic CH), 1642 (stretching C=N), 1603, 1467, 1230 (asymmetric stretching C–O–C). $^1$H NMR ($CDCl_3$, ppm) $\delta$: 14.40 (s, 2H, OH), 8.16 (s, 2H, CH=N), 7.75 (d, 4H, $J$=8.34 Hz, $H^{2',6'}$), 7.63 (s, 2H, $H^6$), 7.25 (d, 4H, $J$=8.34 Hz, $H^{3',5'}$), 4.12 (t, 4H, $J$=6.24 Hz, $OCH_2$), 3.62 (t, 4H, $J$=6.34 Hz, $CH_2^{\alpha}$), 2.64 (t, 4H, $J$=7.62 Hz, Ph–$CH_2$), 2.46 (t, 4H, $J$=6.24 Hz, $CH_2^{\gamma}$), 2.23 (s, 3H, $NCH_3$), 1.91–0.85 (m, 128H, aliphatic protons). The thermal behaviour is reported in table 2.

### 2.2.3. Preparation of $H_2L_3$.

$\mathbf{H_2L_3}$ was prepared by reacting *N*,*N*-bis(3-aminopropyl)methylamine and **III** in

Table 2. Optical and thermal properties of $\mathbf{H_2L_{1-4}}$ ligands. Cr=crystal, Sm=smectic, I=isotropic liquid.

| Ligand | Transition | $T$/°C | $\Delta H$/kJ mol$^{-1}$ |
|---|---|---|---|
| $\mathbf{H_2L_1}$ | Cr–Cr′ | 83.4 | — |
| | Cr′–SmA | 85.0 | 64.1[a] |
| | SmA–I | 96.7 | 17.2 |
| | I–SmA | 62.4 | 15.2 |
| | SmA–Cr | 38.3 | 16.6 |
| $\mathbf{H_2L_2}$ | Hexatic SmX–SmC | | |
| | SmC–I | 45.7[a] | 72.3 |
| | I–SmC | 43.9 | 3.7 |
| | SmC–Hexatic SmX | 40.1 | 48.9 |
| $\mathbf{H_2L_3}$ | Cr–I | 100.0 | 85.0 |
| | I–SmC | 85.7 | 1.4 |
| | SmC–Cr | 72.5 | 60.9 |
| $\mathbf{H_2L_4}$ | Cr–I | 88.2 | 80.5 |
| | I–SmC | 74.9 | 12.5 |
| | SmC–Cr | 69.1 | 46.2 |

[a] Only a broad peak for the two transitions.

methanol (reflux, 4h). The crude product was purified by recrystallization from acetone and then dried *in vacuo* to give a yellow solid; yield 0.47 g (84%). IR (KBr, $cm^{-1}$) *v*: 2923–2852 (stretching aliphatic CH), 1734 (stretching C=O), 1692, 1633 (stretching C=N), 1606, 1266. $^1H$ NMR ($CDCl_3$, ppm) $\delta$: 14.01 (s, 2H, OH), 8.33 (s, 2H, CH=N), 8.12 (d, 4H, $J$=9.15 Hz, $H^{2',6'}$), 7.25 (d, 2H, $J$=8.55 Hz, $H^6$), 6.95 (s, 4H, $J$=9.15 Hz, $H^{3',5'}$), 6.79 (d, 2H, $J$=1.83 Hz, $H^3$), 6.71 (dd, 2H, $J_{3,5}$=1.83 Hz/$J_{5,6}$=8.55 Hz, $H^5$), 4.03 (t, 4H, $J$=6.72 Hz, $OCH_2$), 3.64 (t, 4H, $J$=6.72 Hz, $CH_2^{\alpha}$), 2.45 (t, 4H, $J$=6.72 Hz, $CH_2^{\gamma}$), 2.24 (s, 3H, $NCH_3$), 1.91–1.26 (m, 44H, aliphatic protons), 0.88 (t, 6H, $J$=6.72 Hz, $CH_3$). The thermal behaviour is reported in table 2.

**2.2.4. Preparation of** $H_2L_4$. $\mathbf{H_2L_4}$ was prepared by treating *N*,*N*-bis(3-aminopropyl)methylamine with **IV** in methanol (reflux, 4 h). The crude product was purified by recrystallization from acetone and then dried *in vacuo* to give a yellow solid; yield 0.50 g (88%). IR (KBr, $cm^{-1}$) *v*: 2921–2852 (stretching aliphatic CH), 1730 (stretching C=O), 1635 (stretching C=N), 1608, 1267. $^1H$ NMR ($CDCl_3$, ppm) $\delta$: 13.53 (s, 2H, OH), 8.31 (s, 2H, CH=N), 8.11 (d, 4H, $J$=9.51 Hz, $H^{2',6'}$), 7.13–7.09 (m, 4H, $H^4$ and $H^6$), 7.00–6.93 (m, 6H, $H^3$ and $H^{3',5'}$), 4.03 (t, 4H, $J$=6.33 Hz, $OCH_2$), 3.65 (t, 4H, $J$=6.33 Hz, $CH_2^{\alpha}$), 2.44 (t, 4H, $J$=7.14 Hz, $CH_2^{\gamma}$), 2.23 (s, 3H, $NCH_3$), 1.91–1.27 (m, 44H, aliphatic protons), 0.88 (t, 6H, $J$=6.33 Hz, $CH_3$). The thermal behaviour is reported in table 2.

### 2.3. *Synthesis of* $UO_2L_{1–4}$ *and* $NiL_{1–4}$ *complexes*

**2.3.1. Preparation of** $UO_2L_1$. Uranyl acetate dihydrate (0.09 g, 0.21 mmol), dissolved in ethanol (5 ml), was added to a hot solution of $\mathbf{H_2L_1}$ (0.20 g, 0.21 mmol) in ethanol (15 ml). The reaction mixture was stirred at reflux for 6 h and then cooled to room temperature. The solid product, collected by filtration, was washed with water, then ethanol and recrystallized from chloroform/methanol to give an orange solid; yield 0.24 g (96%). IR (KBr, $cm^{-1}$) *v*: 2924–2853 (stretching aliphatic CH), 1623 (stretching C=N), 1599, 1540, 898 (symmetric stretching $UO_2$). The thermal behaviour is reported in table 3. $^1H$ NMR data are unavailable because of the low solubility.

The homologous compounds $\mathbf{UO_2L_{2–4}}$ were prepared similarly; again, $^1H$ NMR data are unavailable because of low solubility. Colours, yields, melting points, IR data and elemental analyses are reported below.

$\mathbf{UO_2L_2}$: red-orange solid, yield 0.21 g (87%). IR (KBr, $cm^{-1}$) *v*: 2921–2851 (stretching aliphatic CH), 1650 (stretching C=N), 1600, 1466, 1250 (asymmetric stretching C–O–C), 904 (symmetric stretching $UO_2$). The thermal behaviour is reported in table 3.

$\mathbf{UO_2L_3}$: the crude product was recrystallized from chloroform/ethanol to give an orange solid, yield 0.17 g (66%), m.p. 270°$C_{dec}$. IR (KBr, $cm^{-1}$) *v*: 2924–2853 (stretching aliphatic CH), 1733 (stretching C=O), 1644 (stretching C=N), 1591, 1477, 1295, 1255, 894 (symmetric stretching $UO_2$).

$\mathbf{UO_2L_4}$: the crude product was recrystallized from chloroform/ethanol to give a red-orange solid, yield 0.12 g (46%), m.p.>350°C. IR (KBr, $cm^{-1}$) *v*: 2924–2853 (stretching aliphatic CH), 1728 (stretching C=O), 1629 (stretching C=N), 1606, 1483, 1254, 892 (symmetric stretching $UO_2$).

**2.3.2. Preparation of** $NiL_1$. A solution of nickel acetate tetrahydrate (0.05 g, 0.21 mmol) and $\mathbf{H_2L_1}$ (0.20 g, 0.21 mmol) in ethanol (15 ml) was stirred at reflux for 6 h and then cooled to room temperature. The solid was filtered off, washed with water, then ethanol and recrystallized from chloroform/methanol to give a green

Table 3. Optical and thermal properties of $\mathbf{UO_2L_{1–2}}$ and $\mathbf{NiL_{1–2}}$ complexes.

| Complex | Transition | $T$/°C | $\Delta H$/kJ $mol^{-1}$ | $d$/Å |
|---|---|---|---|---|
| $\mathbf{UO_2L_1}$ | Cr–SmC | 180.2 | 20.3 | 39.8 |
| | SmC–$I_{dec}$ | 300 | | |
| $\mathbf{UO_2L_2}$ | Cr–SmC | 53[a] | | 37.6 |
| | SmC–I | 118[a] | | |
| | I–SmC | 113[a] | | |
| | SmC–Cr | 92[a] | | |
| $\mathbf{NiL_1}$ | Cr–I | 104.2 | 110.8 | 39.0 |
| | I–SmC | 74.2 | 4.2 | |
| $\mathbf{NiL_2}$ | Cr–SmC | 41.0 | 68.8 | 42.3 |
| | SmC–I | 120.6 | <1 | |

[a] Data from optical microscopy.

solid; yield 0.19 g (88%). IR (KBr, cm$^{-1}$) $\nu$: 2923–2850 (stretching aliphatic CH), 1634 (stretching C=N), 1603, 1475, 1386. The thermal behaviour is reported in table 3. $^1$H NMR data are unavailable because the compound is a paramagnetic complex.

The homologous compounds $\mathbf{NiL_{2-4}}$ were prepared similarly. Colours, yields, melting points, IR data and elemental analyses are reported below. $^1$H NMR data are unavailable because these compounds are paramagnetic complexes.

$\mathbf{NiL_2}$: red solid, yield 0.14 g (70%). IR (KBr, cm$^{-1}$) $\nu$: 2921–2851 (stretching aliphatic CH), 1636 (stretching C=N), 1592, 1240 (asymmetric stretching C–O–C). The thermal behaviour is reported in table 3.

$\mathbf{NiL_3}$: green solid, yield 0.14 g (67%), m.p. 168–171°C. IR (KBr, cm$^{-1}$) $\nu$: 2922–2852 (stretching aliphatic CH), 1726 (stretching C=O), 1633 (stretching C=N), 1603, 1253.

$\mathbf{NiL_4}$: green solid, yield 0.17 g (78%), m.p. 136–140°C. IR (KBr, cm$^{-1}$) $\nu$: 2917–2851 (stretching aliphatic CH), 1726 (stretching C=O), 1639 (stretching C=N), 1607, 1250.

## 3. Results and discussion

### 3.1. *Synthesis*

The preparation of the $\mathbf{H_2L_{1-4}}$ ligands is accomplished by the condensation of *N*,*N*′-bis(3-aminopropyl)methylamine with the appropriately substituted 2-hydroxybenzaldehydes, **I–IV** (see § 2.2). The $\mathbf{H_2L_{1-4}}$ ligands, obtained in good yields (84–90%), are yellow ($\mathbf{H_2L_1}$, $\mathbf{H_2L_{3-4}}$) and orange ($\mathbf{H_2L_2}$) solids. Analytical data (IR, $^1$H NMR spectra and elemental analyses) are consistent with the expected $\mathbf{H_2L_{1-4}}$ stoichiometry.

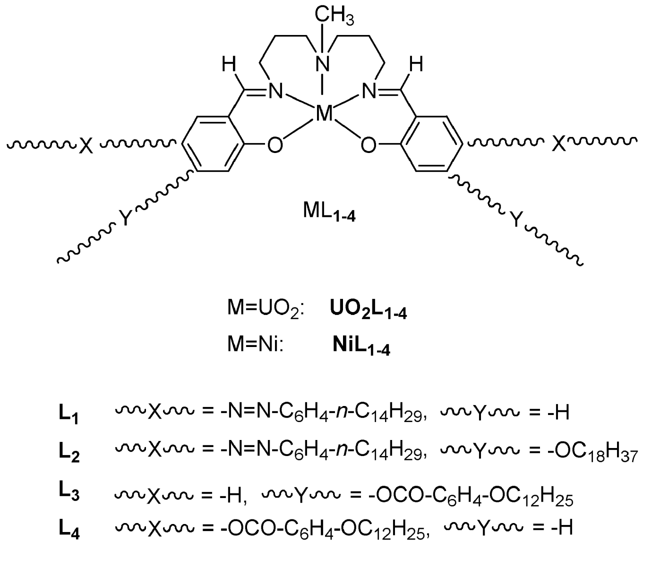

Figure 2. Chemical structure of $\mathbf{UO_2L_{1-4}}$ and $\mathbf{NiL_{1-4}}$ complexes.

The $\mathbf{H_2L_{1-4}}$ chelating species reacted with UO$_2$(II) or Ni(II) salts leading to the metal derivatives $\mathbf{UO_2L_{1-4}}$ and $\mathbf{NiL_{1-4}}$ (see figure 2) whose purity was confirmed by elemental analyses (table 1). The new complexes were characterized by IR spectroscopy, but $^1$H NMR spectra were unavailable because of the low solubility of $\mathbf{UO_2L_{1-4}}$ and the paramagnetic nature of the high spin $\mathbf{NiL_{1-4}}$ complexes. Interestingly, the IR spectra of UO$_2$(II)-containing species showed a typical band of medium intensity in the 895–910 cm$^{-1}$ region, which can be attributed to the symmetric stretching of the UO$_2$(II) group [11].

The coordination geometry adopted by the UO$_2$(II) and Ni(II) cations can be predicted from that of analogous complexes reported in the literature. In particular, with the $\mathbf{UO_2L_{1-4}}$ complexes a heptacoordination can be supposed, where the dioxouranium rod is probably oriented perpendicular to the plane in which the N$_3$O$_2$ set of donating atoms lies [13]. On the other hand, for the paramagnetic high spin $\mathbf{NiL_{1-4}}$ complexes, due to the chelating nature of the N$_3$O$_2$ cavity, the Ni(II) centre is penta-coordinated adopting a TPY geometry with the equatorial positions occupied by the CH$_3$-bonded nitrogen atom and the two oxygen atoms [12].

### 3.2. *Mesomorphism*

The phase sequence, transition temperatures and enthalpy changes of the synthesized species were studied using polarizing optical microscopy (POM), differential scanning calorimetry (DSC) and powder X-ray diffraction (XRD). These results for both the ligands and complexes are summarized in tables 2 and 3, respectively. The azo-containing ligands $\mathbf{H_2L_1}$ and $\mathbf{H_2L_2}$ are found to be thermotropic smectogens. In particular, they exhibited the typical focal conic with myelinic figures ($\mathbf{H_2L_1}$: SmA) and schlieren ($\mathbf{H_2L_2}$: SmC) texture, respectively [15].

XRD studies of $\mathbf{H_2L_2}$ showed that the phase at room temperature is not crystalline. In fact, the diffraction pattern showed a series of four sharp Bragg peaks in the small angle region, with spacings in the ratio 1:2:3:4, accompanied by a relatively sharp peak in the wide angle region, centred at a scattering angle $2\theta$ of about 20.9°. The small angle Bragg peaks (fundamental and first three harmonics) are diagnostic of a well organized layered structure characterized by a periodicity $d$ of 61 Å. The full width at half maximum of the wide angle peak is intermediate between that characteristic of long range positional ordering and that typical of the short range liquid like positional ordering of the disordered Sm phases (A or C), corresponding to a correlation length of about 100 Å. This pattern is consistent with the hexatic SmB phase, or its tilted versions SmF and SmI, which are characterized by the onset of a certain degree of order within the layers, whereas positional coupling between the layers remains extremely weak or totally absent.

In this mesophase the lateral packing of the molecules is locally hexagonal (implying long axis rotation) and the lattice parameter *a* is 4.9 Å. This positional order is not long range and disappears over distances of the order of the correlation length. However, the hexatic phase displays long range lattice orientational order. Based only on the powder XRD and without knowledge of the molecular length (no experimental data are available to estimate the actual length of the forked $\mathbf{H_2L_2}$ molecule), it is not possible to discriminate between the orthogonal (SmB) and the tilted (SmF of SmI) nature of the hexatic mesophase. Moreover, a distinction between these different phases through POM observations was not possible, since $\mathbf{H_2L_2}$ showed a very fine schlieren-like texture, characteristic of all the hexatic phases, even if less common than the mosaic variant [15]. However, since the usual phase transition sequence already reported [16–18] is such that the tilted SmI and SmF appear before the SmC phase while the orthogonal SmB is associated with the SmA phase, it seems possible to deduce, from the phase transition sequence observed in $\mathbf{H_2L_2}$, the tilted nature of the hexatic mesophase.

Both the $\mathbf{H_2L_3}$ and $\mathbf{H_2L_4}$ ligands exhibited a monotropic SmC phase, stable over a temperature range of some 10°C (table 2).

Coordination compounds containing the azo moiety, $\mathbf{UO_2L_1}$, $\mathbf{UO_2L_2}$, $\mathbf{NiL_1}$ and $\mathbf{NiL_2}$, displayed liquid crystalline properties (table 3), whereas none of the complexes containing $\mathbf{H_2L_3}$ and $\mathbf{H_2L_4}$ ligands (i.e. $\mathbf{UO_2L_3}$, $\mathbf{UO_2L_4}$, $\mathbf{NiL_3}$ and $\mathbf{NiL_4}$) were mesomorphic. All the mesogenic metal complexes showed a SmC phase, characterized by a schlieren texture and, upon cooling from the isotropic liquids, all retained the mesophase texture giving a glassy solid stable up to one month. The nature of the SmC phase, identified by POM, was successfully confirmed by XRD.

## 4. Conclusions

A new series of ligands containing a $N_3O_2$ chelating cavity ($\mathbf{H_2L_{1-4}}$) has been synthesized, all show smectic mesophases. A comparison of the mesomorphic behaviour between the ligands is not significant, considering that the substituents on the salycilidene phenyl rings are different in the series (figure 1). However, it should be noted that only the ligands bearing the azo moieties ($\mathbf{H_2L_1}$ and $\mathbf{H_2L_2}$) showed enantiotropic mesomorphism. As expected, the transition temperatures are found to be sensitive to the number and position of the alkyl chains, and strongly decrease for $\mathbf{H_2L_2}$, in which two lateral tails are present. Moreover, when the salycilidene phenyl rings are substituted with ester moieties, the corresponding ligands $\mathbf{H_2L_3}$ and $\mathbf{H_2L_4}$ display only monotropic mesomorphism with clearing temperatures ($T_c$) correlated to the position of the ester substituents; $T_c$ ($\mathbf{H_2L_4}$)<$T_c$ ($\mathbf{H_2L_3}$).

Finally, with regards to the central core, no comparisons are possible with the previously reported bissalicylidenediamino ligands bearing the same peripheral groups [9, 10] and containing a $N(CH_2)_nN$ ($n$=2 or 3) bridge, because of the extremely different geometry of the group connecting the two salycilidene fragments, $N(CH_2)_3N(CH_3)N(CH_2)_3N$ present in the new ligands, to $\mathbf{H_2L_1}$ and $\mathbf{H_2L_2}$.

The reaction of $\mathbf{H_2L_{1-4}}$ with $UO_2$(II) or Ni(II) salts resulted in the corresponding metal derivatives $\mathbf{UO_2L_{1-4}}$ and $\mathbf{NiL_{1-4}}$. The expected molecular geometry around the $UO_2^{2+}$ cation is such that the *c.n.* is seven and the dioxouranium rod is perpendicular to the plane on which all the metal-bonded $N_3O_2$ atoms lie. By contrast, the nickel complexes are penta-coordinated high spin paramagnetic species, wherein the $N(CH_2)_3N(CH_3)N(CH_2)_3N$ bridge probably spans equatorial and axial positions in a distorted TPY coordination polyhedron.

Interestingly, the results of the present investigation proved that the strong pro-mesogenic capacity of the phenylazo-containing peripheral tails in salicylidenediaminate ligands is able to induce mesomorphic behaviour in metal complexes regardeless of the Ni(II) coordination geometry. Indeed, upon complexation of the new $\mathbf{H_2L_{1-4}}$ ligands, the mesomorphism is stabilized for derivatives bearing azo substitutents ($\mathbf{H_2L_{1-2}}$), all showing the SmC phase, regardless of the nature of the metallic centre, while for the $\mathbf{H_2L_{3-4}}$ ligands the presence of the ester groups, independent of the molecular shape of the resulting complex (roughly bent for $\mathbf{H_2L_3}$ or linear for $\mathbf{H_2L_4}$) prevented the formation of metallomesogenic species.

In conclusion, it may be noted that, to the best of our knowledge, these newly synthesized species are the first hepta-coordinated $UO_2$(II) and penta-coordinated paramegnetic Ni(II) metallomesogens reported to date.

## Acknowledgements

This work was partly supported by the Italian Ministero dell'Istruzione, dell'Università e della Ricerca (MIUR) through the INSTM-FIRB and Centro di Eccellenza CEMIF.CAL grants.

## References

[1] B. Donnio, D. Guillon, R. Deschenaux, D.W. Bruce. *Comprehensive Coordination Chemistry II*, Vol. 6, J.A. McCleverty, T.J. Meyer (Eds), Elsevier, Oxford (2003).

[2] K. Binnemans, C. Görller-Walrand. *Chem. Rev.*, **102**, 2303 (2002).

[3] L. Ziminski, J. Malthête. *Chem. Commun.*, 1495 (1990).

[4] E. Terazzi, J.-M. Bénech, J.-P. Rivera, G. Bernardinelli, B. Donnio, D. Guillon, C. Piguet. *Dalton Trans.*, 769 (2003).

[5] F. Morale, R.W. Date, D. Guillon, D.W. Bruce, R.L. Finn, C. Wilson, A.J. Blake, M. Schroder, B. Donnio. *Chem. Eur. J.*, **9**, 2484 (2003).

[6] A.G. Serrette, T.M. Swager. *J. Am. chem. Soc.*, **115**, 8879 (1993).

[7] R.W. Date, E.F. Iglesias, K.E. Rowe, J.M. Elliott, D.W. Bruce. *Dalton Trans.*, 1914 (2003).

[8] M. Ghedini, D. Pucci, A. Crispini, G. Barberio. *Organometallics*, **18**, 2116 (1999).

[9] I. Aiello, M. Ghedini, F. Neve, D. Pucci. *Chem. Mater.*, **9**, 2107 (1997).

[10] I. Aiello, M. Ghedini, M. la Deda, D. Pucci, O. Francescangeli. *Eur. J. inorg. Chem.*, 1367 (1999).

[11] L. Sacconi, I. Bertini. *J. Am. chem. Soc.*, **88**, 5180 (1966).

[12] M. Di Varia, P.L. Orioli, L. Sacconi. *Inorg. Chem.*, **10**, 553 (1971).

[13] U. Cesellato, M. Vidali, P.A. Vigato. *Inorg. Chim. Acta*, **77**, 18 (1976).

[14] J.-P. Bayle, E. Bui, F. Perez, J. Courtieu. *Bull. Soc. chim. Fr.*, **4**, 532 (1989).

[15] I. Dierking. *Textures of Liquid Crystals*. Wiley-VCH, Weinheim (2003).

[16] D. Rogez, J.L. Gallani, P. Martinoty. *Phys. Rev. Lett.*, **80**, 1256 (1998).

[17] C. Nagabhushan, G.G. Nair, B.R. Ratna, R. Shashidar, J.W. Goodby. *Liq. Cryst.*, **3**, 175 (1988).

[18] C.C. Huang, G. Nounesis, R. Geer, J.W. Goodby, D. Guillon. *Phys. Rev. A, rapid Commun.*, **39**, 3741 (1989).